SINGLE-CHANNEL CURRENTS FROM ACETYLCHOLINE RECEPTORS IN EMBRYONIC CHICK MUSCLE

Kinetic and Conductance Properties of Gaps Within Bursts

ANTHONY AUERBACH AND FREDERICK SACHS
Department of Biophysical Sciences, State University of New York, Buffalo, New York 14214

ABSTRACT In tissue-cultured chick muscle, bursts of current from single nicotinic ion channels contain a variety of low-conductance gaps. One population has a lifetime of ~0.1 ms and an unknown conductance. A second population has a lifetime of 2–10 ms and conductance of zero. The third population has a lifetime of 0.5–1 ms and a mean conductance ~2% that of the main conductance state. This subconductance state has an agonist-dependent lifetime, longer for suberyldicholine than for acetylcholine, and is liganded to the same extent as the main conductance state. Subconductance gaps have a linear current-voltage behavior in the range −60 to −140 mV and appear to have the same reversal potential as the main state. The subconductance state is composed of a group of states which interconvert with correlation times longer than 300 μs.

INTRODUCTION

When single-channel currents from nicotinic acetylcholine receptors were first observed by Neher and Sakmann (1976), the currents appeared as rectangular pulses of equal amplitude. With increases in the time and amplitude resolution of the patch-clamp technique (Hamill et al., 1981), the structure of the single-channel currents has been recognized to be more complex. Channel openings were observed to occur in clusters, or "bursts" (Nelson and Sachs, 1979). This bursting had been predicted by Colquhoun and Hawkes (1977) and suggested by Sakmann and Adams (1979) for a three-state kinetic model. A number of groups have analyzed nicotinic ion-channel activity using three- or four-state reactions (Colquhoun and Sakmann, 1981; Dionne and Leibowitz, 1982; Leibowitz and Dionne, 1983; Nelson and Sachs, 1981; Sine and Steinbach, 1983).

A more intricate picture of burst structure developed when Hamill and Sakmann (1981) noticed that nicotinic channels in tissue-cultured rat muscle could adopt multiple, discrete conductance states. The subconductance state (~10 pS) was easily observed at low temperatures, where it had a lifetime of several milliseconds. The reversal potential and selectivity of the subconductance state were indistinguishable from those of the main open state. Hamill and Sakmann also made the rather surprising observation that transitions between the subconductance state and the main state were not in equilibrium. Subconductance sojourns occurred following bursts, but not before bursts. In contrast to these results, Trautmann (1982) reported that transitions to and from the subconductance state appeared to be in equilibrium, although his experiments were done with different agonists and at room temperature.

Auerbach and Sachs (1983) observed that in tissue-cultured chick muscle, gaps within bursts were heterogeneous, consisting of at least two conductance populations (0% and 10% of the open channel conductance) and another kinetically distinct population (time constant <0.1 ms) of undetermined conductance. Because not all gaps have zero current, they cannot represent the closed, liganded state used in the kinetic analyses mentioned above.

In addition to showing a discrete subconductance state, Hamill and Sakmann's data (1981) showed substantial fluctuations of the subconductance current about its mean. These fluctuations are suggestive of additional states, perhaps similar to those reported by Sigworth (1981) for the main conducting state of the channel.

In the present study we have characterized the gaps within and adjacent to bursts in order to gain a physical understanding of what controls transitions to and from the various states within bursts. The results indicate that the subconductance state is actually an ensemble of states having an average conductance ~12% that of the main conductance state and a lifetime that depends on the agonist. There is a distinct population of relatively long-lived gaps whose mean current is effectively zero. Gaps within bursts do not involve ligand dissociation. The data show that transitions to and from the subconductance state are close to equilibrium.

METHODS

Pectoral muscles from 10–12 d chick embryos were dissected and dissociated in divalent cation-free saline containing 2 mg/ml Type IV

collagenase (Sigma Chemical Co., St. Louis, MO). The cells were counted in trypan blue and then plated in gelatin-coated 60-mm plastic culture dishes at a density of 10^6 cells/dish. The cells were grown in a tisse-culture medium containing Dulbecco's modified Eagle's medium (DMEM); 10% heat-inactivated horse serum (both from Grand Island Biological Supply, Grand Island; NY); 2% homemade embryo extract; penicillin; and streptomycin. Cells were incubated at 37°C in an atmosphere of 5% CO_2 and 95% air saturated with water vapor. After ~2 d in culture, the medium was changed to one containing 10^{-5} M cytosine arabinoside (Sigma) for 30 h to inhibit fibroblast growth. The experiments were performed on cells grown in culture 6–14 d. For recording, the growth medium was replaced with saline containing 140 mM NaCl, 4 mM KCl, 2 mM $CaCl_2$, 1 mM $MgCl_2$, and 10 mM Na HEPES (pH 7.4).

Patch pipettes were made from borosilicate glass capillaries and coated with Sylgard (Dow Corning, Midland, MI) according to Hamill et al. (1981). The patch amplifer was similar to that desciribed by Hamill et al., except that we used a Burr-Brown OPA-101 amplifier for the current-to-voltage converter. The 3 db bandwidth of the system was >10 kHz. All experiments were done on cell-attached patches. The agonists were acetylcholine (ACh), 50–100 nM, and suberyldicholine (SubCh), 5–10 nM. The temperature was 22–24°C.

Data were recorded on analog magnetic tape and then transferred to digital tape at a sampling rate of 20 kHz. The anti-aliasing filter was a four-pole Bessel set at 8 kHz. The bandwidth was further limited by a finite-impulse–response (FIR) digital filter which had a Gaussian response in both the time and frequency domains (Colquhoun and Sigworth, 1983). The effective bandwidth of our analyses ranged from 2–6 kHz. The data were analyzed by an automated pattern-recognition program (Sachs et al., 1982) which utilized a half-amplitude threshold-crossing criterion to identify transitions and a pattern-matching algorithm to reject noise. The baseline estimate was updated approximately every 25 ms. We arbitrarily defined bursts as a series of channel openings separated by gaps shorter than 7 ms.

To measure amplitudes accurately, we had to reject data that included the effects of amplifier-filter settling. We rejected all data within a "dead time" preceding and following each transition. This dead time was set equal to $0.6/f_c$, where f_c is the 3-db bandwidth. Thus, at 5 kHz our dead time allowance was three samples (150 μs) and our total allowance for settling and delays was 300 μs, so that we analysed only gaps that were 350 μs or longer. The half-amplitude method for measuring event durations is biased for events that are less than $\sim 0.5/f_c$ (Sachs and Auerbach, 1983). Therefore, when fitting histograms of event durations, we imposed a dead-time allowance similar to that used for amplitude analysis.

We estimated event amplitudes in two ways. First, each data point (exclusive of the settling/delay allowance) was entered into an amplitude histogram which we will call a total-current histogram. Second, we computed the mean of the data points within each gap and stored this value with the corresponding gap duration. From these data we compiled histograms of mean amplitude and/or duration.

Curve fitting was done with a general-purpose nonlinear least-squares algorithm. Histograms were fit to the integral of the appropriate probability density function evaluated over each bin. This allowed for variable bin widths and prevented the finite bin width from biasing the fit. To allow for the Poisson distribution of counts in each bin, the squared residuals were weighted inversely with the number of counts in each bin (Bevington,1969). To avoid biasing the fit when the histogram was sparse, bin widths were adjusted so that each bin contained at least five counts (Sachs and Auerbach, 1983). For signal-averaged transitions (see below) the data points were equally weighted. Except where otherwise noted, confidence limits are "support plane" estimates at the 90% level (Marquardt, 1964). These are symmetrical confidence limits on a parameter independent of the errors in the other parameters.

Histograms of mean gap amplitude presented a special problem because the variance of each measurement depended upon the event duration. Amplitudes of long events were more precise than those of short events. For these data the sample variance was inversely proportional to the number of data points in the average. Therefore, for these data, in addition to the standard histogram weighting procedure, the residuals were weighted in proportion to the number of raw data points contributing to each bin. Thus weighted, the variance of a Gaussian fitted to the mean amplitude distribution is dominated by the variance of the underlying population and not the measurement errors. This population variance included a component from intrinsic variability of the conductance and a component from errors in the baseline estimation.

We wanted to estimate the kinetics of subconductance gaps separately from zero current gaps. We fit the amplitude-duration data to a statistical model where the mean amplitude of each event was assumed to be drawn from one of two Gaussian distributions and where the duration of events in each amplitude distribution was described by an exponential probability density function. The variance of the amplitude distribution was taken to be a sum of the population variance (σ_p^2) and the single-sample, wideband variance (σ_s^2) normalized by the number of data points used to calculate the mean amplitude of the event (N),

$$\sigma^2 = \sigma_p^2 + \sigma_s^2/N. \quad (1)$$

Thus, the joint probability density of obtaining an event of amplitude a and duration d was given by

$$P(a,d) = k \exp(-kd) \times (1/\sigma\sqrt{\pi})\exp\{-0.5([a - \langle a \rangle]/\sigma)\}^2 \quad (2)$$

where (σ) has been taken from Eq. 1 above, $\langle a \rangle$ is the mean of the appropiate amplitude distribution, and k is the mean of the appropriate duration distribution. In practice, the time distribution has to be normalized to cover the actual range of the data, rather than the usual range from zero to infinity. The relevant distribution means and variances were estimated as described above.

We then used the maximum likelihood technique to fit the two time constants. The likelihood of observing a particular set of N events is

$$L = \prod_{i=1}^{N} P(x_i),$$

where $P(x_i)$ is the probability of observing event x_i (Bevington, 1969). L, actually log L, was maximized with respect to the parameters by using a Newton-type algorithm. We tested that the suspected maximum was indeed global by generating multiple random starting points. Approximate confidence limits were obtained by holding one parameter constant and then changing the other until the likehood fell to the requisite level. Thus, a 90% confidence interval would correspond to a set of parameters that make the data set 10% as likely.

To estimate the likelihood of passage through a subconductance state preceding and following bursts, we aligned the leading and trailing edges of bursts at the moment of threshold crossing and analysed the average current. When subconductance sojourns are present, these burst transitions are preceded and followed by exponential phases that reflect the lifetime of the subconductance sojourn. The amplitude of the decay (or rise) extrapolated to the moment of threshold crossing is the product of the amplitude of the subconductance current and the probability of passing through a subconductance state. We curve fit the average current tails to single exponentials with an offset to allow for slight differences in the estimation of baselines before and after bursts.

RESULTS

Kinetic Characteristics of Gaps Within Bursts

Fig. 1 shows several bursts of current from channels activated by acetylcholine in which subconductance gaps

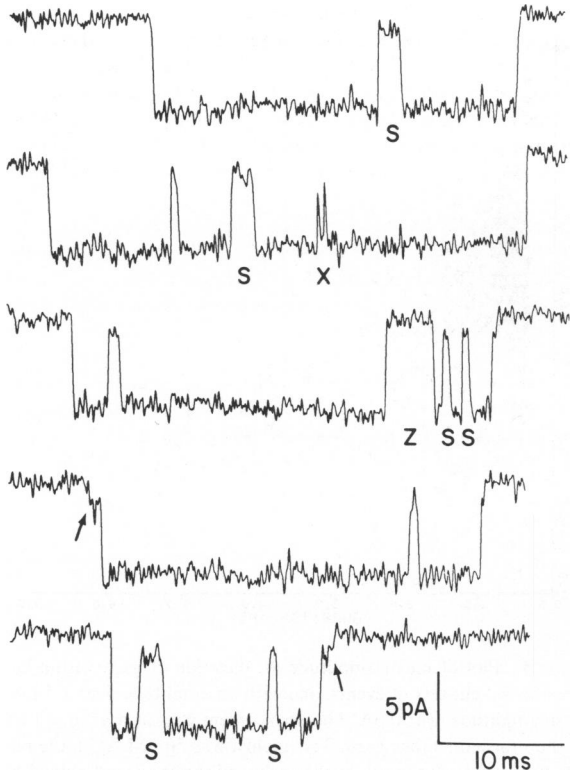

FIGURE 1 Examples of gaps within bursts of nicotinic channel currents. The gaps fall into one of three categories: those with zero current (Z), those with nonzero current (S for subconductance), and those too short to have amplitudes that could be determined (X). Most of the burst edges rise and fall cleanly from the baseline. In the lower two traces, subconductance sojourns on the leading and trailing edges of bursts are marked with arrows. The agonist was 50 nM ACh, the pipette was held at 80 mV relative to the bath, and the data were analyzed at a bandwidth of 3.0 kHz.

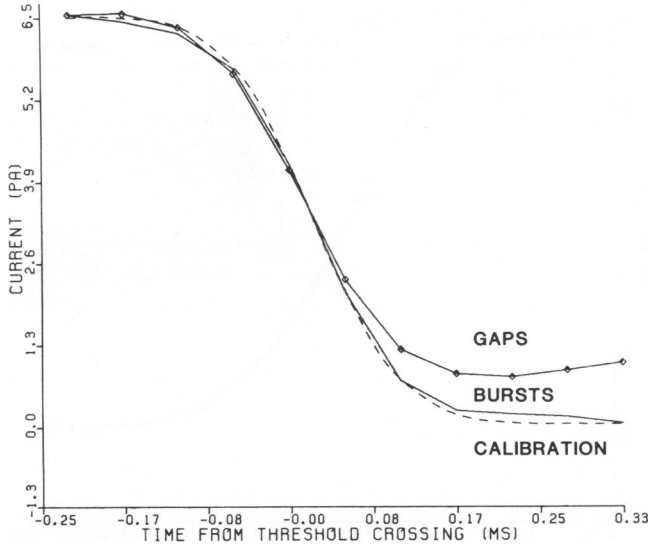

FIGURE 2 A comparison of the mean closing-transition amplitudes of gaps within bursts (connected symbols) and burst trailing edges (solid line, —). Inward current is shown upward. For reference, a calibration trace from a capacitively-coupled triangle wave is included (dashed line, ---). The appropriate transitions were aligned at the moment of threshold crossing and were signal-averaged. Only intraburst gaps longer than 450 μs were included in the average, accounting for the rather flat mean gap amplitude. The transition amplitude of gaps within bursts is less than that of burst terminations (gaps between bursts). Analysis of the distribution of gap mean amplitudes (cf., Fig. 5) showed that in this record, over 90% of the gaps within bursts were from a subconductance population. The experimental conditions are the same as Fig. 1.

are clearly visible. Isolated examples such as these cannot be taken as proof of subconductance sojourns because the overlap of gap current with baseline noise or with independent channel currents can produce gaps having nonzero current. A statistical analysis of gap amplitudes shows , however, that a large percentage of the gaps that appear during bursts do have a current greater than zero (Auerbach and Sachs, 1983). The result is graphically illustrated in Fig. 2, where we have aligned and averaged the edges of several hundred gaps within and between bursts. The mean amplitude of the current step was smaller for gaps within bursts than for gaps between bursts. The transition times are similar to the calibration pulse (dotted line). In the record shown, the fraction of bursts that terminated through a subconductance state was small, because the average burst trailing edge closely resembles the response of the amplifier.

As an independent test of our methods of analysis, we examined the amplitude characteristics of gaps produced by the local anesthetic QX-222 in nicotinic channels, and gaps present in Ca^{++}-activated K^+-channel currents (Fig. 3). The amplitude of virtually all gaps from both types of channel was zero.

Our methods for estimating the amplitudes and durations of conductance events are illustrated in Figs. 4–6 for one sample data set. The channels were activated by 50 nM ACh. Recall that in these figures, event amplitudes were measured only after allowing for amplifier and filter settling.

Fig. 4 shows a scatter plot of mean gap amplitude vs. duration for 483 events, 0.35–7.0 ms in length. Two amplitude distributions are visible, one close to zero and the other near 1.5 pA. Although not shown, a similar scatter plot of the main open channel amplitude vs. duration showed only a single distribution.

The two components of the amplitude distribution are shown more clearly in Fig. 5, where the mean gap amplitudes have been compiled into a histogram. The means, based on a sum of Gaussians fit to the histogram, were 0.01 ± 0.07 pA and 1.28 ± 0.12 pA. A similar analysis of the open channel scatter plots yielded a unitary current of 6.23 ± 0.01 pA. The standard deviation of the subconductance population (0.49 ± 0.15 pA) was significantly greater than that of the zero current population (0.23 ± 0.08 pA). From the areas under each distribution, 75% of the events were from the subconductance population.

We also estimated the mean currents of the two popula-

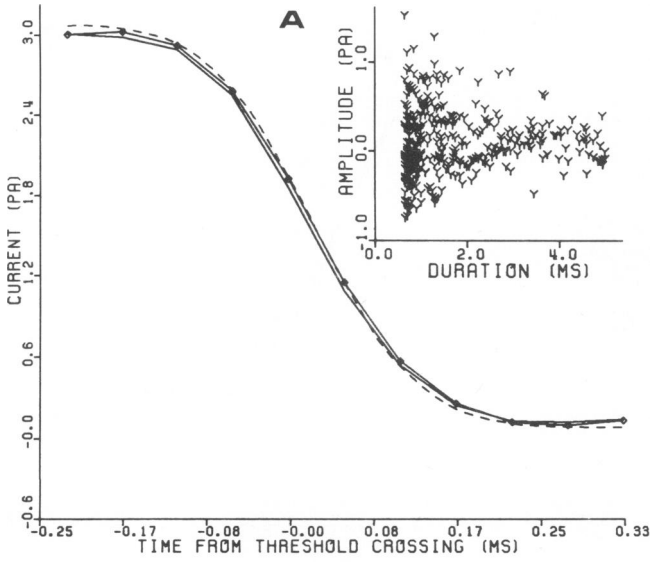

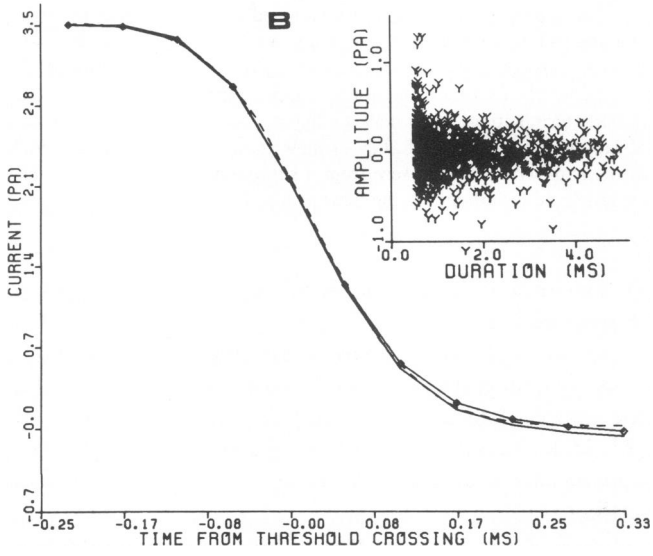

FIGURE 3 Mean closing transitions of gaps within and between bursts from nicotinic channels blocked by QX-222 (*A*, inward current up) and from Ca^{++} channels (*B*, outward current up). The notation is the same as in Fig. 1. The *insets* show the mean amplitude/duration cross correlations for gaps 0.6 ms or longer. In both experiments, virtually all of the gaps within bursts had zero current. In the QX-222 experiment (*A*), the pipette contained 10 nM SubCh and 20 μM QX-222. In the K^+ channel experiment (*B*), the pipette contained normal saline only and was held at -60 mV relative to the bath. The bandwidth of the analyses was 2.0 kHz.

tions from the amplitude histogram of all data points within gaps (Fig. 6). The data points of this distribution are equally weighted. Fitting this total-current histogram with the sum of two Gaussians yielded means for the zero current and subconductance population at -0.09 ± 0.05 pA and 1.43 ± 0.08 pA. From the areas under each distribution we estimated that only 39% of the data points were contributed by subconductance gaps.

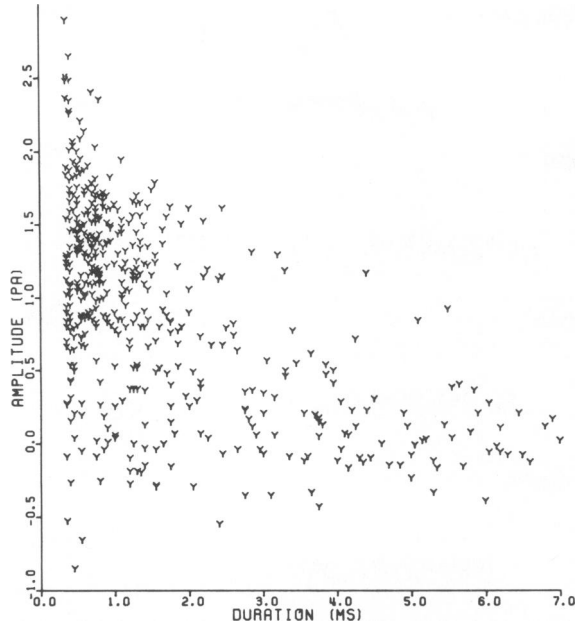

FIGURE 4 Plot of mean amplitude vs. duration of gaps within bursts. There are two clusters of events, one with an amplitude near 1.5 pA and with an amplitude near 0 pA. The zero current gaps appear to last longer than the subconductance gaps. The agonist was 50 nM ACh, the pipette was held at +80 mV relative to the bath, and the analysis bandwidth was of 5.0 kHz.

The observation that a majority of the events but a minority of the data points came from subconductance gaps is evidence that zero-current gaps are longer than subconductance gaps. This difference in duration can be seen in the scatter plot of Fig. 4, where at long times there are proportionally fewer events of the subconductance

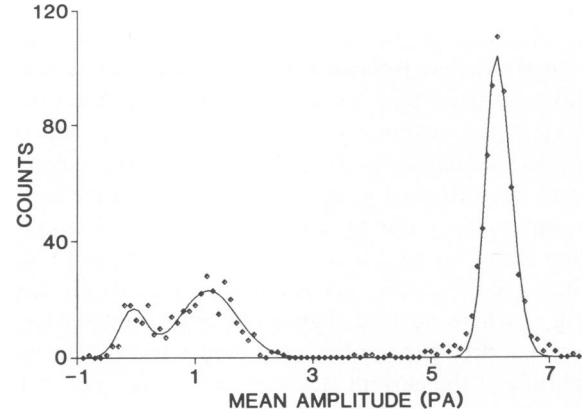

FIGURE 5 Histogram of the mean amplitudes of events within bursts. Three distinct populations can be distinguished. Openings to the main conductance state had an average current of 6.2 pA, subconductance gaps had an average current of 1.3 pA, and zero current gaps had an average current of 0.0 pA. Of the low conductance events, an estimated 75% were from the subconductance population. The data for events whose amplitude was less than half the open channel current were compiled from the scatter plot shown in Fig. 4. The data for the main conductance state came from a similar analysis. Note that the distribution variance is greatest for the subconductance population. The bandwidth of the analysis was 3.0 kHz.

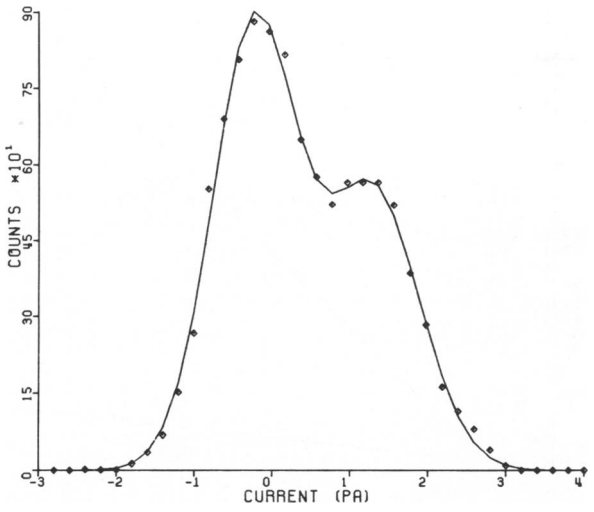

FIGURE 6 Histogram of the amplitude of data points within gaps. The effects of amplifier and filter settling were eliminated by excluding data points preceding and following transitions. Two populations are apparent, one near 1.4 pA and the other near 0 pA. 39% of the data points belong to the higher-current population. The data are from the same record as Fig. 4. The bandwidth was 3.0 kHz.

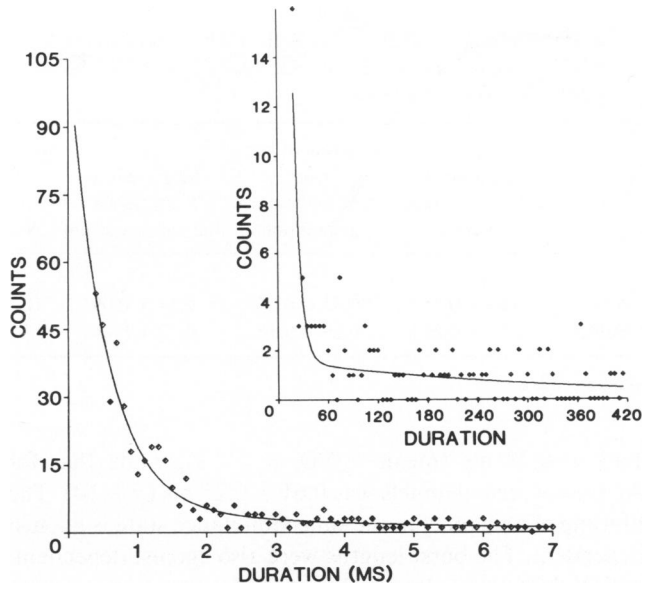

FIGURE 7 Histogram of the durations of gaps within bursts. The data were compiled from the scatter plot shown in Fig. 4. In the range 0.45 to 7.0 ms, the data were fit to the sum of two exponentials with characteristic time constants of 0.5 and 6.9 ms (—). The maximum likelihood method of determining the subconductance population lifetime gave an estimate of 0.6 ms, suggesting that there is a close correlation of the substate lifetime with the shorter of the two time constants measured from the unconditional distribution of gap durations. The *inset* shows the distribution of long closed periods (primarily of gaps between bursts) fit to a sum of two exponentials (—). The shorter time constant component corresponds to the 6.9 ms component of intraburst gaps. The time constant of the longer component was 340 ms.

amplitude. We used the maximum-likelihood technique described in Methods to quantify the kinetic difference between the subconductance and zero current populations. For simplicity, we assumed that the lifetime of each amplitude distribution could be described by a single exponential. Using the amplitude means and variances described above as fixed parameters, and fitting the two time constants, we found that for the experiment shown in Fig. 4 the subconductance population had a lifetime of 0.66 ± 0.14 ms while the zero-current population had a lifetime of 6.45 +13.5/−3.2 ms. The wide confidence limits on the time constant of the zero-current population reflect the fact that few of the zero-current events occurred within the 7 ms closed-time limit we used to define a burst.

These time constants were compared with the time constants estimated from an unconditional histogram of closed times. In the range 0.5 to 7.0 ms the data were described by the sum of two exponentials. For the experiment shown in Fig. 7, the time constant of the faster process was 0.58 ± 0.16 ms and that of the slower process was 6.85 ± 2.02 ms, with an estimated 77% of the events belonging to the short time-constant population. Thus, there is an excellent agreement between the results from the maximum likelihood analysis and the unconditional distribution. This agreement supports our assumption that there is only a single kinetic component to the population of subconductance gaps.

Could the zero current gaps be associated with interburst closed periods, i.e., those times which were likely to have included sojourns to an unliganded state? A histogram of durations longer than 20 ms is shown in the *inset* of Fig. 7. The time constant of the slow component was 340 ms (109 events). We expect only two events from this distribution shorter than 7 ms, while we measured over 100 such zero current gaps. Thus, we can say that the zero current gaps within bursts are not from the same distribution as are the long, interburst closed periods. Our estimates of the lifetime of gaps with zero current varied but remained in the range of 2–10 μs.

In addition to the two intraburst closed periods described above there was a third component of very short gaps which had a lifetime of ~0.1 ms. Because the lifetime of this population was too short to permit precise amplitude measures, we have no information about whether this component represented transitions to a subconductance or to a zero current state. The fraction of all gaps belonging to this population was quite variable, accounting for <10% to >80% of all gaps within bursts. This variability was consequently reflected in the channel open time. These brief gaps may represent sojourns to a doubly-liganded, closed state as per Colquhoun and Sakmann (1981); transient blockage by a diffusible substance present at concentrations >10 μM; or simply another short-lived conformational state with a low conductance.

We used the maximum-likelihood method to examine the agonist dependence of the lifetime of subconductance gaps. The results for ACh and SubCh are described in Table I. For SubCh-activated channels the lifetime was

TABLE I
AGONIST DEPENDENCE OF THE AMPLITUDE AND KINETIC PROPERTIES OF SUBCONDUCTANCE GAPS WITHIN BURSTS

	Lifetime of subconductance gaps	Fraction of gaps from subconductance population	Amplitude as a fraction of main state current	*N*
	ms			
ACh	0.61 ± 0.25	0.84 ± 0.20	0.11 ± 0.09	10
SubCh	1.13 ± 0.28	0.79 ± 0.16	0.12 ± 0.04	12

(mean ± SD).

1.13 ± 0.28 ms (mean ± SD, $n = 12$), while that for ACh-activated channels was 0.61 ± 0.25 ms ($n = 10$). The lifetime of a channel in the subconductance state is agonist dependent. The burst lengths were also agonist dependent, with SubCh bursts longer than ACh bursts.

We find that in tissue-cultured embryonic chick pectoral muscle there are at least two types of nicotinic channel which can be distinguished on the basis of main open state conductance. One type has a conductance of 50 pS and the other type a conductance of 35 pS. This observation parallels those from other tissue-cultured systems (cf. Hamill and Sakmann, 1981; Trautmann, 1982). To test whether the lifetime of subconductance gaps was different for the two channel types, we split the data set for ACh-activated channels according to the main state conductances. For the 50-pS channel, the gap lifetime was 0.59 ± 0.12 ms ($n = 4$) and for the 35-pS channel the gap lifetime was 0.62 ± 0.32 ($n = 6$). The subconductance-state lifetime appears to be the same in both channel types.

The subconductance-state lifetime also did not depend on the membrane potential over the range of −66 to −140 mV.

Is there an agonist dependence to the probability of a channel entering a subconductance (as opposed to a zero current) state within a burst? We compared the relative areas under the two peaks fit to the gap mean amplitude histogram (cf., Fig. 5) for ACh- and SubCh-activated channels. The results are shown in Table I. There was substantial scatter in the data from different patches. For 35-pS channels activated by SubCh, the fraction of subconductance gaps ranged from 0.43 to 0.97. Over all experiments, regardless of agonist, channel conductance, or voltage, the fraction of subconductance gaps was 0.81 ± 0.18 (mean ± SD), but with no clear indication of agonist or voltage dependence to this value.

Amplitude Characteristics of Gaps Within Bursts

Fig. 8 shows the current-voltage (*I-V*) relationship for both subconductance and main conductance states of SubCh-activated channels. Within the accuracy limits of the technique, both classes of event showed a linear *I-V* relationship, corresponding to conductances of 4 and 33 pS. The extrapolated reversal potentials for the main and the subconductance state were 0 mV and −15 mV, assuming a resting potential of −72 mV. This difference of 15 mV was not statistically significant. In many patches we could not obtain sufficient data to determine the *I-V* relationship precisely, so we chose to express the subconductance gap current as a fraction of the unitary current. Over all experiments, the subconductance gap current was 12 ± 5 % of the unitary current. The ratio of substate to main state current ranged from 0.06 to 0.23, with no apparent agonist dependence (Table I).

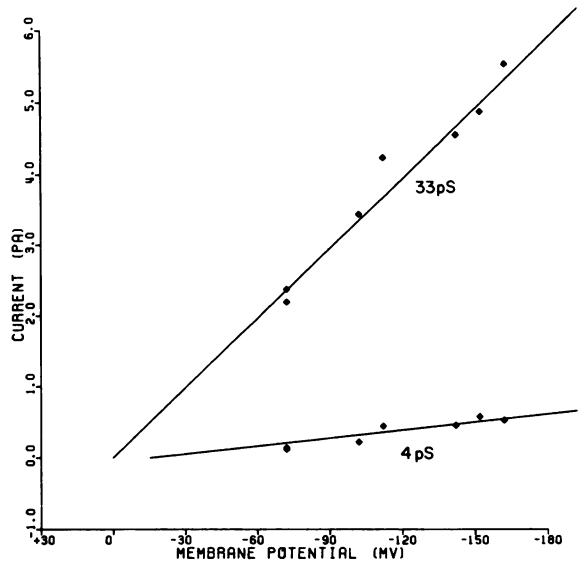

FIGURE 8 Current-voltage relationship of the open channel and of subconductance gaps. The estimates of event current were obtained by fitting mean amplitude histograms to Gaussians (see Figs. 4 and 5). The estimates of membrane potential were obtained by assuming a zero-current potential of 0 mV for the main conductance state. The current-voltage relationship was fit to a straight line with the residuals weighted inversely with the 90% confidence limits on the current amplitude estimates. The conductance of the main open state was 33 pS and that of the subconductance state was 4 pS. The extrapolated reversal potential of the subconductance state was 15 mV hyperpolarized to that of the main conductance state, and the estimated cell resting potential was 72 mV. The data came from three separate patches from the same region of a single cell. The agonist was 5 nM SubCh.

Current Fluctuations of Events Within Bursts

As mentioned above, when the histogram of mean gap amplitude is fit to a sum of Gaussians, the variance of the subconductance component is substantially greater than that of the zero current component. This observation suggests that the subconductance state is in fact an ensemble of states. To estimate the spectral characteristics of this excess variance, we measured variances of events at five different bandwidths. For example, in the experiment corresponding to Fig. 5 (3 kHz bandwidth), the variances

were baseline (gaps between bursts), 0.38 pA^2; main open channel current, 0.53 pA^2; subconductance gaps, 0.57 pA^2; and zero-current gaps, 0.45 pA^2. In Fig. 9 we have plotted the excess variance (signal variance minus baseline variance) for the open channel, the subconductance gaps and the zero current gaps as a function of the data bandwidth. For reference, Fig. 9 includes the Lorentzian distribution function given by a $\tan^{-1}$ function). The distribution function rises to a maximum, equal to the total variance, reaching half maximum at the cutoff (3db) frequency.

The subconductance gap fluctuations are rather long lived, compared to those of open channels, persisting for mean times greater than 0.3 ms. These data are consistent with the results of Hamill and Sakmann (1981), which showed increased noise of the substate relative to both the fully closed and open states.

Equilibrium Properties of Bursts

Hamill and Sakmann (1981) proposed that transitions between the main state and the subconductance state are not in equilibrium. They reported that the probability of a substate preceding a burst is much less than the probability of a substate following a burst. As one measure of equilibrium, we aligned and averaged the leading and trailing edges of bursts. In this form, subconductance sojourns preceding bursts appeared as an exponential buildup of current, while those following bursts appeared as an exponential decay. An example of such an analysis is shown in Fig. 10. Fitting an exponential to the falling phase of the burst trailing edge gave an estimate of a process with a time constant of 0.60 ± 0.20 ms. A similar fit to the leading edge of the burst (shown time-reversed in Fig. 10) gave a time constant estimate of 0.55 ± 0.15 ms. In the same record, the lifetime of subconductance gaps was 1.08 ms. The intercepts of the exponential phases with the point of threshold crossing is the product of the subconductance current and the probability of passing through the subconductance state. For the experiment shown in Fig. 10, the intercept of the rising phase was 0.6 ± 0.1 pA and that for the falling phase was 0.5 ± 0.1 pA. The substate current derived from the histogram of mean gap amplitudes was 0.40 ± 0.03 pA. Assuming that the current amplitudes of inter- and intraburst subtrates are equal virtually all bursts began and ended with subconductance sojourns. For comparison, in this record, over 90% of all gaps within bursts were to a subconductance state.

Compared with intraburst substate gaps, the probablitiy of occurrence of substates on burst edges was highly

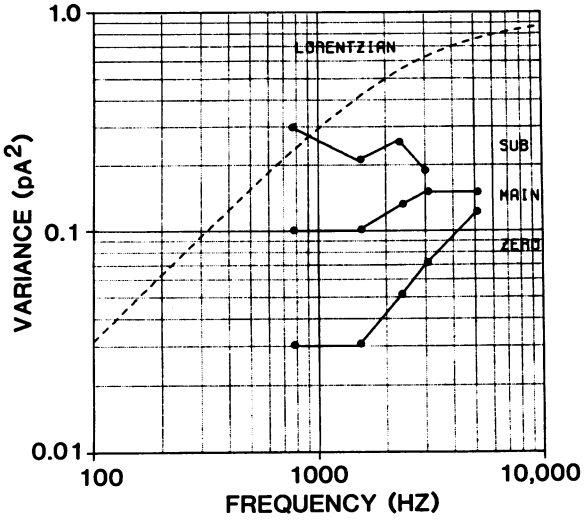

FIGURE 9 The spectral distribution function of the current fluctuations of events within bursts. Each curve represents the integral of the variance up to the frequency indicated. The dotted line (---) shows what a Lorentzian power spectrum looks like in this format (cutoff frequency at 5 kHz). The *SUB* trace represents fluctuations in subconductance gaps, whose mean current in this experiment was ~1.3 pA. The *MAIN* trace represents the fluctuations of the main open state, whose amplitude was ~6.2 pA. The plot indicates a cutoff at ~2.5 kHz for the main open state, which is the same as that observed from conventional power spectra (Auerbach and Sachs, unpublished observations). The *ZERO* trace represents the fluctuations of those gaps within bursts that had a mean current close to zero. The most pronounced feature of this trace is the strong frequency dependence suggestive of opening processes with durations shorter than 50 μs (taken from the same record as Fig. 4).

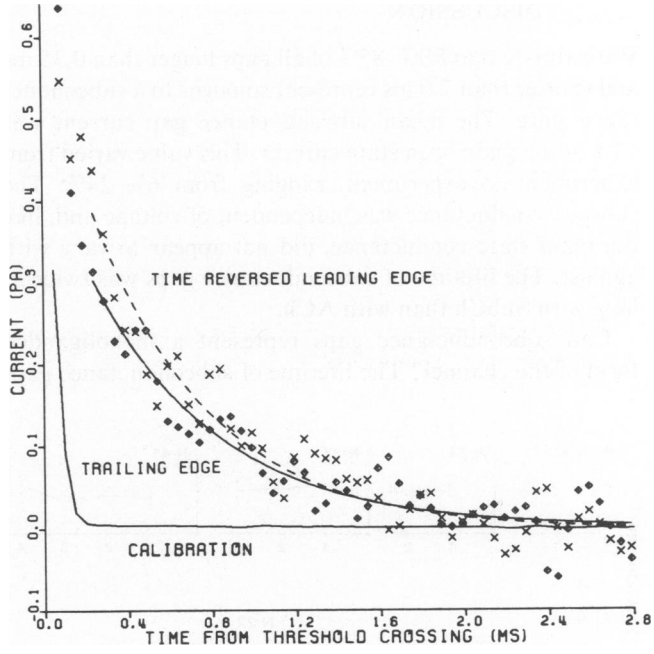

FIGURE 10 Signal-averaged leading and trailing edges bursts. When substantial numbers of subconductance sojourns are present before and after bursts, exponential phases of current precede and follow the mean burst transitions. The open channel current was 3.83 pA, far off scale. The averaged trailing edges (♦ and —) and leading edges (*X* and --- , shown time-reversed) were each fit to a single exponential from 350 μs to 2.8 ms after (or before) crossing half amplitude. The amplifier/filter response to a capacity coupled triangle wave is shown in the trace labeled *CALIBRATION*. The fitted curves are similar with regard to time constant and area, indicating that the foward and reverse rates are close to being in equilibrium. As an index of variability, compare these results with those shown in Fig. 2 where few subconductance sojourns were observed on burst edges. The agonist was 5 nM SubCh.

variable. Some records showed virtually no exponential phase either preceding or following bursts (compare Figs. 2 and 10). There was a tendency for the exponential phases of current preceding and following bursts to be faster, by about a factor of two, than the lifetime of intraburst substate gaps. Nonetheless, when exponentials were clearly visible, the time constants and intercepts of the currents before and after bursts did not differ by more than a factor of two, with no trend as to which was larger. Transitions to and from the subconductance state appear to be close to equilibrium.

If transitions into bursts were out of equilibrium, we might expect that the open states would be out of equilibrium. To test this, we measured the duration of events in bursts as a function of position within the burst. Symmetric variations in this parameter are kinetically interesting but do not indicate lack of equilibrium (Colquhoun and Hawkes, 1982), while asymmetric variations do indicate a lack of equilibrium. Fig. 11 shows the results for one record in which there were a large number of events so that the standard deviations of the durations were small. In all records there was no correlation, either symmetric or asymmetric, of the open time with position in the burst.

DISCUSSION

We estimate that 80%–85% of all gaps longer than 0.35 ms and shorter than 7.0 ms represent sojourns to a subconductance state. The mean subconductance gap current was 12% of the main open state current. This value varied from experiment to experiment, ranging from 6%–24%. The substate conductance was independent of voltage and, like the main state conductance, did not appear to vary with agonist. The lifetime of subconductance gaps was twice as long with SubCh than with ACh.

Can subconductance gaps represent a monoliganded form of the channel? The lifetime of subconductance gaps

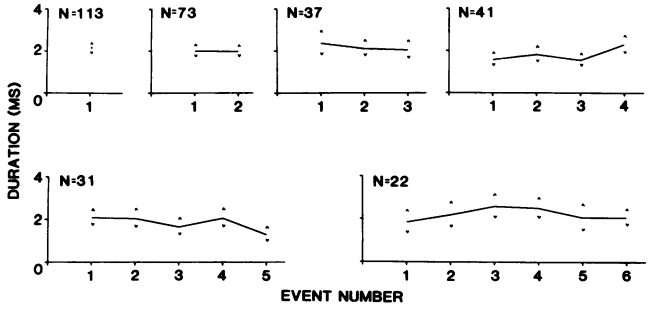

FIGURE 11 The mean duration of channel open times as a function of position with bursts. All bursts of 1, 2, 3...etc. events were separately collected and the durations of corresponding events were averaged and plotted as a function of position within the burst. The standard deviations for each mean are indicated by the arrows. The number of bursts contributing to each mean are indicated in the figure. The fact that there is no asymmetry in the durations suggests that the channel closing rates are in equilibrium throughout a burst. The experimental conditions were the same as in Fig. 4.

for SubCh-activated channels was ~1 ms. Assuming a diffusion-controlled binding rate of 10^9 s^{-1} M^{-1}, and an agonist concentration of 10 nM, the rate of gaining a ligand would be 10^1 s^{-1}, equivalent to a lifetime of 100 ms. Thus the subconductance state must be liganded to the same extent as the main open state. The same argument holds for the other classes of gaps within bursts.

The subconductance state appears to be heterogeneous, as the variance of the subconductance gap current is consistently larger than the current variances of the baseline, the zero current gaps, and the main conductance state. Furthermore, the excess variance (over the baseline) did not vary with bandwidth in the range from 0.75–3.0 kHz. (The frequency range was limited on the low end because few events persisted long enough to permit filter settling, and on the high end because noise resulted in threshold crossings which prematurely terminated the gaps).

Can a two-state model account for the excess variance? Suppose that within a subconductance gap there are sojourns to zero-current (gaps within gaps). The mean ($\langle I \rangle$) and variance (σ^2) of the subconductance gap current would be given by: $\langle I \rangle = ap$, $\sigma^2 = a^2p(1 - p)$, where a is the true subconductance current amplitude and p is the probability that during a gap the channel carries current a (Lecar and Sachs, 1981). In the example shown in Figs. 4–7 the amplitude of the subconductance current was 1.28 pA and the excess variance was ~0.25 pA^2. Solving two equations above we found that $a = 1.43$ pA and $p = 0.90$.

For a simple two-state system with opening rate k_o and closing rate k_c, $p = k_o/(k_o + k_c)$, $\tau = 1/(k_o + k_c)$, where τ is the relaxation time constant. Because the variance was constant over the range 0.75–3.0 kHz, $\tau > 320$ μs, $k_o < 2.8$ 10^3 s^{-1} and $k_c < 0.3 \times 10^3 s^{-1}$. This means that the excess variance could arise if the true subconductance current were 1.43 pA and if it were interrupted by complete closures longer than 360 μs at intervals longer than 3 ms. In the experiment corresponding to the above calculation, the subconductance gap lifetime was 0.6 ms. Thus, most subconductance events would not contain a closure and should therefore have a variance approximately equal to that of the baseline. In fact, the population variance of subconductance gaps appeared to be independent of event duration (Fig. 9). We therefore conclude that a simple two-state model of gaps within gaps is wrong and that there are more than two components to the substate. The mechanism that accounts for the excess fluctuations in the substate current may also account for the fluctuations in the open channel current (Sigworth,1981, and above). More complete analyses of spectra are necessary to determine whether fluctuations arise from current variations within each gap or from heterogeneity between gaps.

As with subconductance gaps, the variance of the zero-current gaps is greater than the baseline. The result indicates that the mean current cannot actually be zero, although it is indistinguishable from zero in our experi-

ments. Because the spectral distribution function for zero-current gaps (Fig. 9) does not level off by 5 kHz, these fluctuations must arise from a process, or processes, having correlation times <30 μs. The excess variance might arise from openings which are too brief to reach the detection threshold. At 5 kHz, events shorter than ~40 μs do not reach threshold (Sachs and Auerbach, 1983). The two-state analysis used above predicts that the observed excess variance could be explained by full channel openings shorter than 30 μs occurring at intervals of 1.9 ms. These kinetics predict a mean current of 0.1 pA, close to the accuracy limits of our experiments.

The drop in conductance associated with the subconductance state implies a change in the rate-limiting step(s) to permeation. Because the subconductance state current and the reversal potential follow the main state, the change in permeation rates does not appear to involve a change in a single energy barrier (Hille, 1975). In our experiments, the *I-V* relationship of subconductance gaps was linear. If a single barrier were to become rate limiting, the *I-V* relationship would be expected to approach an exponential, although it is not clear how much deviation from linearity would be apparent over the range of voltages we have used. A simple phenomenological interpretation of the subconductance state is that a well in the free energy profile for permeation is transiently deepened, producing a fivefold drop in conductance but no change in selectivity. It is intriguing that both the lifetime of the subconductance state and the burst length are similarly influenced by the agonist, suggesting that the ion-binding site and the gate may be identical.

Like Trautmann (1982), we found no evidence that either the main conductance or the subconductance states of the channel are far from equilibrium. Our measurements showed that within a factor of two, forward and backward reactions occur with equal frequency. We have observed deviations greater than the apparent experimental error, but not in a consistent direction. In no case did the deviations approach the level of 2^{39} reported by Hamill and Sakmann (1981). We have no explanation for the difference in results, with the possible exception that the temperature in Hamill and Sakmann's experiments was significantly lower (8°C) than either ours or Trautmann's . It would be surprising, however, to find such a dramatic temperature dependence to the reaction unless there were some form of phase transition.

We thank Rich McGarrigle for cell preparation and other technical assistance, and Jim Neil for computer programming which maximized the likelihood of this work.

This work was supported by grant NS-13194 from the United States Public Health Service.

Received for publication 6 May 1983 and in final form 10 June 1983.

REFERENCES

Auerbach, A., and Sachs, F. 1983. Flickering of a nicotinic ion channel channel to a subconductance state. *Biophys. J.* 42:1–10.

Bevington, R. P. 1969. Data Reduction and Error Analysis for the Physical Sciences. McGraw-Hill Publications, New York.

Colquhoun, D., and A. G. Hawkes. 1977. Relaxations and fluctuations of membrane currents that flow through drug operated channels. *Proc. R. Soc. Lond. B. Biol. Sci.* 199:231–262.

Colquhoun, D., and A. G. Hawkes. 1981. On the stochastic properties of single ion channels. *Proc. R. Soc. Lond. B. Biol. Sci.* 211:205–235.

Colquhoun, D., and A. G. Hawkes. 1982. On the stochastic properties of bursts of single ion channel openings and clusters of bursts. *Proc. R. Soc. Lond. B. Biol. Sci.* 300:1–59.

Colquhoun, D., and B. Sakmann. 1981. Fluctuations in the microsecond time range of the current through single acetylcholine receptor ion channels. *Nature (Lond.).* 294:464–466.

Colquhoun, D., and F. Sigworth. 1983. Analysis of single channel data. *In* Single Channel Recording in Biological Membranes. B. Sakmann and E. Neher, editors. Plenum Publishing Corp., New York. In press.

Dionne, V. E., and M. D. Leibowitz. 1982. Acetylcholine receptor kinetics: a description from single channel currents at snake neuromuscular junctions. *Biophys. J.* 39:253–261.

Hamill, O. P., and B. Sakmann. 1981. Multiple conductance state of single acetylcholine receptor channels in embryonic muscle cells. *Nature (Lond.).* 294:462–464.

Hamill, O. P., A. Marty, E. Neher, B. Sakmann, and F. J. Sigworth. 1981. Improved patch-clamp techniques for high-resolution current recording from cells and cell-free membrane patches. *Pflügers Arch. Eur. J. Physiol.* 391(2,pt.2):85–100.

Hille, B. 1975. Ionic selectivity, saturation and block in sodium channels. *J. Gen. Physiol.* 66:535–560.

Lecar, H., and F. Sachs. 1981. *In* Membrane noise analysis. Excitable Cells in Tissue Culture. P. Nelson and M. Lieberman, editor. Academic Press, New York.

Leibowitz, M., and V. E. Dionne. 1983. Kinetics of endplate acetylcholine receptor single channel currents. *Biophys. J.* 41:134 *a.* (Abstr.)

Marquardt, D. W. 1964. Least squares estimation of nonlinear parameters. IBM Share Library number 3094:15–20.

Neher, E., and B. Sakmann. 1976. Single channel currents recorded from membrane of denervated frog muscle fibres. *Nature (Lond.).* 260:799–802.

Nelson, D. J., and F. Sachs. 1979. Single ionic channels observed in tissue-cultured muscle. *Nature (Lond.).* 282:861–863.

Nelson, D. J., and F. Sachs. 1982. Agonist and channel kinetics of the nicotinic acetylcholine receptor. *Biophys. J.* 37:321*a.*

Sachs, F. and Auerbach, A. (1983). Single channel electrophysiology: use of the patch clamp. *In* Methods in Enzymology: Neuroendocrine Peptides. M. Conn, editor. Academic Press, Inc., New York. In press.

Sachs, F., J. Neil, and N. Barkakati. 1982. The automated analysis of data from single ionic channels. *Pflügers Arch. Eur. J. Physiol.* 395:331–340.

Sakmann, B., and P. R. Adams. 1979. Biophysical aspects of agonist action at frog endplate. *Adv. Pharm. Therap.* 1:81–90.

Sigworth, F. J. 1982. Fluctuations in the current through open ACh-receptor channels. *Biophys. J.* 37:309 *a.* (Abstr.)

Sine, S. M., and J. H. Steinbach. 1983. Apparent channel opening and agonist dissociation rates of the acetylcholine receptor on BC3H1 cells. *Biophys. J.* 41:133 *a.* (Abstr.)

Trautmann, A. 1982. Curare can open and block ionic channels associated with cholinergic receptors. *Nature (Lond.).* 298:272–275.